

# Conformational Flexibility as a Tool for Enabling Site-Selective Functionalization of Unactivated $sp^3$ C–O Bonds in Cyclic Acetals

Ciro Romano,<sup>⊥</sup> Laura Talavera,<sup>⊥</sup> Enrique Gómez-Bengoá, and Ruben Martin\*



Cite This: *J. Am. Chem. Soc.* 2022, 144, 11558–11563



Read Online

ACCESS |



Metrics & More



Article Recommendations

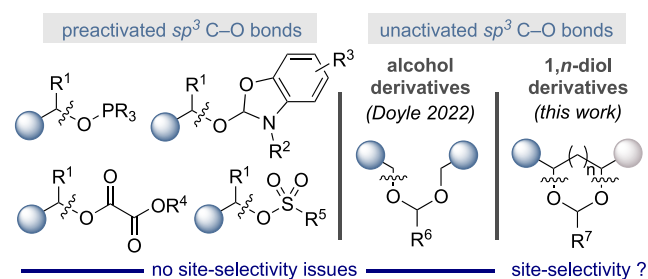


Supporting Information

**ABSTRACT:** A dual catalytic manifold that enables site-selective functionalization of unactivated  $sp^3$  C–O bonds in cyclic acetals with aryl and alkyl halides is reported. The reaction is triggered by an appropriate  $\sigma^*$ –p orbital overlap prior to  $sp^3$  C–O cleavage, thus highlighting the importance of conformational flexibility in both reactivity and site selectivity. The protocol is characterized by its excellent chemoselectivity profile, thus offering new vistas for activating strong  $\sigma$   $sp^3$  C–O linkages.

Carbon–oxygen electrophiles have recently gained momentum as alternatives to organic halides in the cross-coupling arena.<sup>1</sup> Although the use of  $sp^2$  C–O derivatives has become routine, cross-couplings of unactivated  $sp^3$  C–O counterparts possessing  $\beta$ -hydrogens have received much less attention. While significant progress has been made with  $sp^3$  C–O electrophiles bearing electron-withdrawing groups adjacent to the oxygen atom, the  $sp^3$  C–O functionalization of unactivated alkyl ethers—arguably the simplest derivatives in the alcohol series—still remains a challenging endeavor in both two- and one-electron manifolds (Scheme 1).<sup>2–6</sup> This is

## Scheme 1. $sp^3$ C–O Electrophiles in Cross-Coupling Events

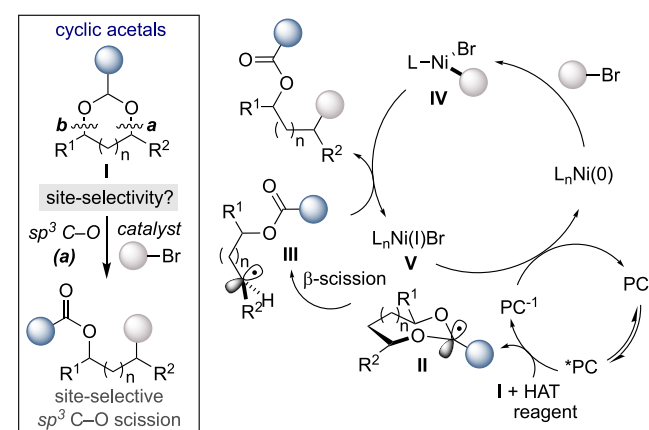


probably attributed to (a) the lower tendency of alkyl ether residues to formally act as leaving groups, (b) the remarkably high activation barrier required for effecting alkyl  $sp^3$  C–O cleavage ( $\sim 93$  kcal·mol<sup>−1</sup>),<sup>7</sup> and (c) inevitable site-selectivity issues arising from the functionalization at both alkyl  $sp^3$  C–O sites.

In recent years, metallaphotoredox scenarios have offered new conceivable pathways to challenging transformations under exceptionally mild conditions.<sup>8</sup> Driven by this observation, we wondered whether we could harness cyclic acetals as vehicles to enable site-selective functionalization of strong  $\sigma$  alkyl  $sp^3$  C–O bonds. Unlike the elegant advances realized with symmetrical acyclic acetals,<sup>9</sup> the utilization of cyclic congeners not only would improve the atom economy of the overall transformation by preserving the integrity of the

organic skeleton but also offer the possibility to discriminate between three similar  $sp^3$  C–O sites, thus constituting a worthwhile endeavor for chemical invention. In addition, the ready availability of cyclic acetals from simple exposure of carbonyl compounds to 1,*n*-diols would offer a unique opportunity for valorization of the latter ubiquitous motifs.<sup>10</sup> We anticipated that a light-driven hydrogen atom transfer (HAT) might occur selectively at the weak acetal  $sp^3$  C–H bond ( $\sim 86.8$  kcal·mol<sup>−1</sup>).<sup>11</sup> Subsequently,  $\beta$ -fragmentation would occur from II via an appropriate  $\sigma^*$ –p orbital overlap, enabling  $sp^3$  C–O cleavage while delivering an open-shell species III (Scheme 2). The latter can be intercepted by Ni(II) species IV, setting the basis for C–C bond formation via

## Scheme 2. Cyclic Acetals as Manifolds for $sp^3$ C–O Cleavage



Received: April 28, 2022

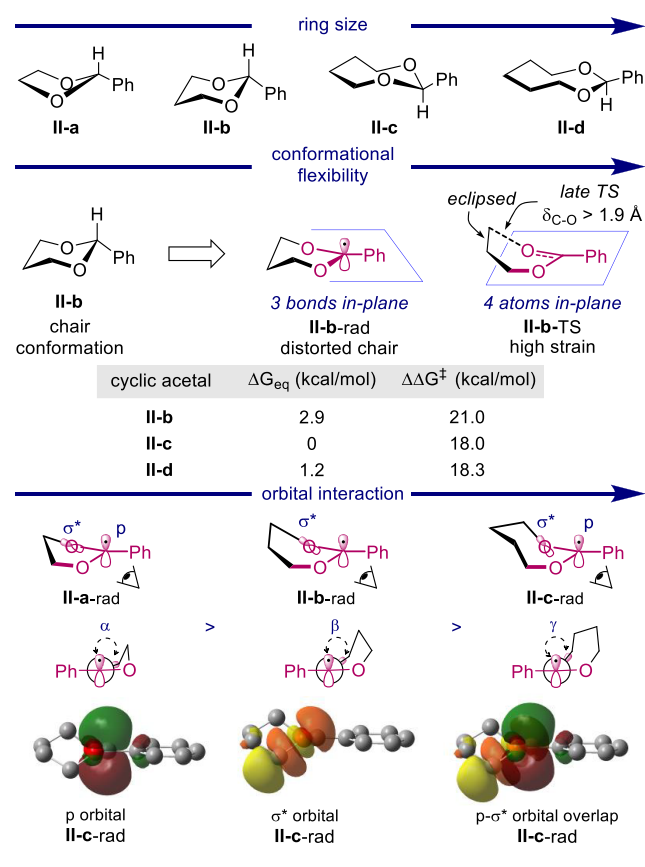
Published: June 24, 2022



reductive elimination. It is expected that the two catalytic cycles could be interfaced by a SET, thus recovering back the propagating catalytic species.

We anticipated that  $\beta$ -fragmentation would only be accessible if a certain degree of conformational flexibility is granted in **II** for enabling the key  $\sigma^*$ -p orbital overlap (Scheme 2). This hypothesis was assessed by DFT calculations on the phenyl-substituted 5- to 8-membered cyclic acetal series (Scheme 3, **IIa-d**).<sup>12</sup> As illustrated for **II-b**, a significant

Scheme 3. DFT Studies; M06-2X/6-311++G(d,p)



buildup of ring strain is observed as the reaction proceeds, either at the radical intermediate (**II-b-rad**) or at the highly strained transition state (**II-b-TS**). Notably, a non-negligible 2.9 kcal·mol<sup>-1</sup> stabilization was observed for **II-c-rad** when compared to **II-b-rad**, probably due to the distortion of the chair in the latter to accommodate the planar radical  $sp^2$  carbon. A close inspection into the fragmentation transition state **II-b-TS** is particularly illustrative, as it confirms the difficult planarization of four atoms in a six-membered ring and a nonfavorable eclipsed conformation of the CH<sub>2</sub>-CH<sub>2</sub> fragment. In addition, the late character of the transition state is associated with a long  $sp^3$  C-O bond (*ca.* 2.0 Å), which introduces an extraordinary distortion in such a small ring. These observations were indirectly corroborated by a significant energy increase of 2.7–3.0 kcal·mol<sup>-1</sup> in **II-b-TS** when compared to **II-c-TS** or **II-d-TS** (Scheme 3, middle). Not surprisingly, we were not able to locate **II-a-TS** due to the exceptional strain that might be built up in smaller ring sizes. Taken together, DFT calculations confirmed conformational flexibility as a key contributory factor for success in our targeted  $sp^3$  C-O cleavage event. As part of our ongoing

interest in light-induced processes and C-O bond functionalization,<sup>13</sup> we describe the realization of this goal. Our method is characterized by its simplicity and generality across a wide number of acetals and organic halides, thus constituting an opportunity to improve our ever-growing knowledge for the activation of particularly strong  $\sigma$   $sp^3$  linkages.

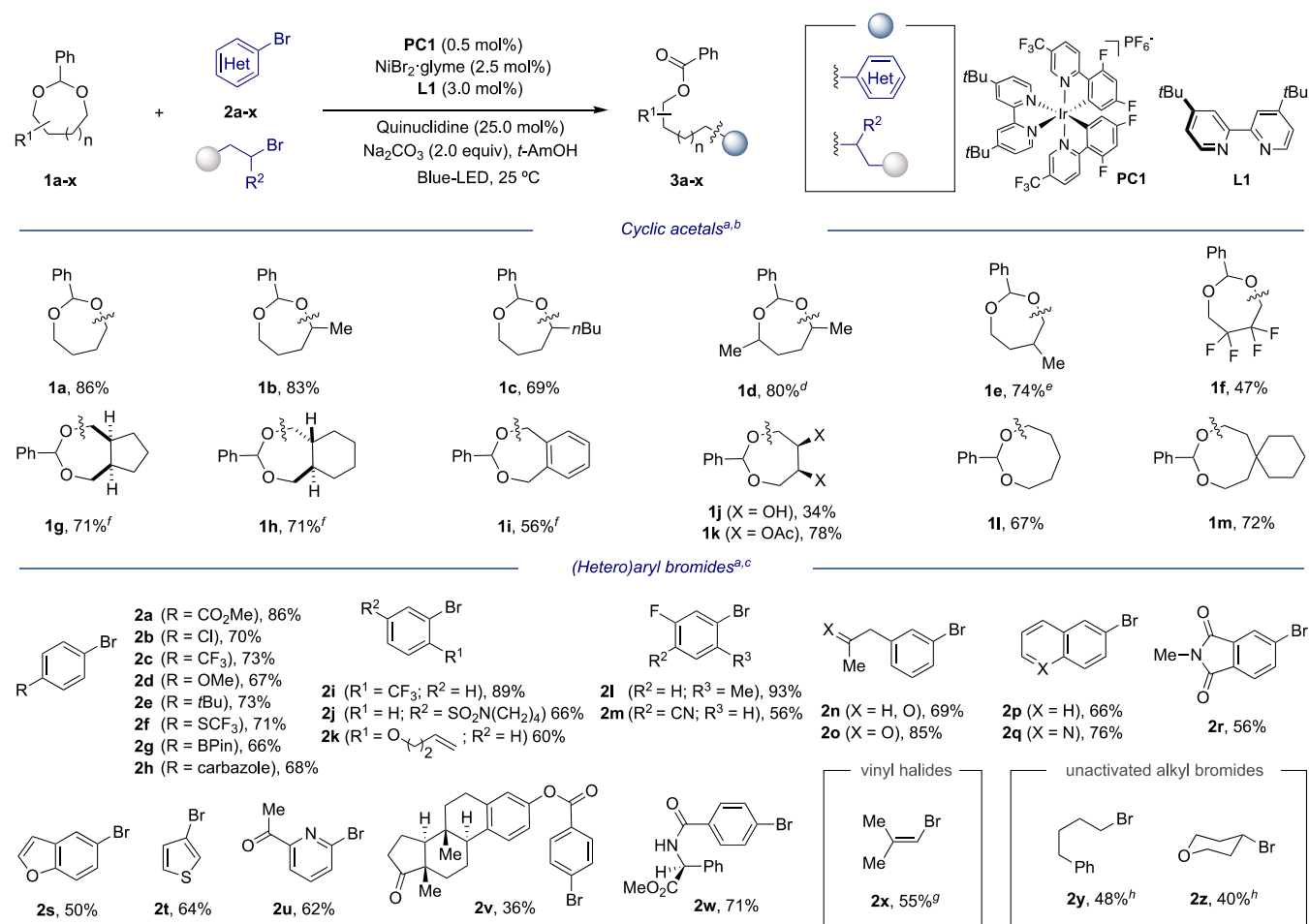
As anticipated from the DFT studies in Scheme 3, all our efforts to promote the  $sp^3$  C-O arylation of either **II-a** or **II-b** (Scheme 3) were met with failure, corroborating the inability of five- and six-membered rings to enable the key  $\sigma^*$ -p orbital overlap.<sup>14</sup> Therefore, our study continued by investigating the reaction of more flexible seven-membered analogue **1a**—readily accessible on a large scale by reaction of 1,4-butanediol with benzaldehyde dimethyl acetal—with **2a** (Table 1). After

Table 1. Optimization of Reaction Conditions<sup>a</sup>

entry	deviation standard conditions	<b>3a</b> (%) <sup>b</sup>
1	none	85 <sup>c</sup>
2	using <b>PC2</b> , <b>PC3</b> or Ru(bpy) <sub>3</sub> <sup>2+</sup>	0
3	using NiI <sub>2</sub>	0
4	using Ni(cod) <sub>2</sub>	70
5	using Cs <sub>2</sub> CO <sub>3</sub>	38
6	using K <sub>3</sub> PO <sub>4</sub>	49
7	MeCN as solvent	33
8	C <sub>6</sub> H <sub>6</sub> as solvent	63
9	using <b>L2</b> as ligand	73
10	using <b>L3</b> as ligand	66
11	using <b>L4</b> as ligand	11
12	using <b>2a-Cl</b> as substrate	49
13	no quinuclidine	65
14	no light, no NiBr <sub>2</sub> ·glyme or no <b>PC1</b>	0

<sup>a</sup>Conditions: **1a** (0.40 mmol), **2a** (0.20 mmol), **PC1** (0.5 mol %), NiBr<sub>2</sub>·glyme (2.5 mol %), **L1** (3.0 mol %), Quinuclidine (25.0 mol %), Na<sub>2</sub>CO<sub>3</sub> (0.40 mmol), *t*-AmOH (0.20 M) under Blue-LED irradiation, 25 °C for 16 h. <sup>b</sup>GC yields using decane as internal standard. <sup>c</sup>Isolated yield.

some experimentation,<sup>15</sup> a protocol consisting of NiBr<sub>2</sub>·glyme, **L1**, quinuclidine, and Ir[(dF,CF<sub>3</sub>ppy)<sub>2</sub>(dtbbpy)]PF<sub>6</sub> in *t*-AmOH under blue-LED irradiation afforded **3a** in 85% isolated yield (entry 1). Notably, no byproducts arising from  $sp^3$  C-H arylation adjacent to the oxygen atoms in **1a** were detected in the crude mixtures.<sup>11</sup> As expected, subtle changes in both photocatalyst and Ni sources had a deleterious effect (entries 2–4). Similarly, solvents and bases other than Na<sub>2</sub>CO<sub>3</sub> and *t*-AmOH resulted in lower yields of **3a** (entries 5–8). Importantly, **3a** was observed in the absence of quinuclidine

Table 2. Site-Selective  $sp^3$  C–O Arylation and Alkylation of Cyclic Acetals

<sup>a</sup>As for Table 1, entry 1. <sup>b</sup>Using **2a** (0.2 mmol). <sup>c</sup>Using **1a** (0.4 mmol); <sup>d</sup>*dr* 1:1. <sup>e</sup>*rr* 2:1. <sup>f</sup>35 °C, 48 h. <sup>g</sup>[Ni] (5.0 mol %), dtbbpy (6.0 mol %). <sup>h</sup>PC1 (1 mol %), [Ni] (10 mol %), dtbbpy (12 mol %), benzene (0.2 M), 5 Å MS (30 mg), 48 h. Isolated yields, average of two different independent runs.

(entry 13), thus suggesting the involvement of bromine radicals ( $BDE_{\text{HBr}} = 86.7 \text{ kcal}\cdot\text{mol}^{-1}$ ) as HAT reagents.<sup>9,16</sup> While in lower yields, non-negligible reactivity was found with **2a-Cl** instead. As anticipated, no product formation was observed in the absence of light, photocatalyst, or Ni catalyst (entry 14).

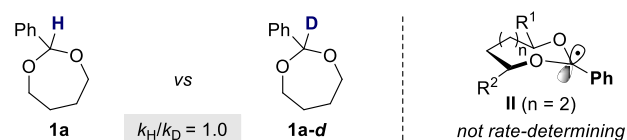
Next, we focused our attention to exploring the generality of our  $sp^3$  C–O functionalization of cyclic acetals (Table 2). As shown, nonsymmetrical 1,3-dioxepanes **1b** and **1c** posed no problems, with arylation taking place exclusively at the more substituted  $sp^3$  C–O site (**3b–c**). Although a lower regioselectivity pattern (2:1) was observed for 5-substituted 1,3-dioxepane **1d**, it is worth noting that the major isomer resulted from the activation at C4, suggesting a certain stabilization of the corresponding open-shell intermediate by hyperconjugation (**3d**).<sup>17</sup> Equally interesting was the ability to couple disubstituted 1,3-dioxepanes or their corresponding ring-fused analogues, obtaining the targeted products **3f–k** in good yields. Despite the presence of five different  $sp^3$  C–H bonds in **1i** amenable for HAT, **3i** was prepared in good yields. While **3j** was obtained in a low 34% yield, a simple esterification of the pending hydroxyl moieties led to **3k** in good yields. These results should be visualized against the challenge that is addressed due to the presence of seven

nucleophilic carbinolic  $sp^3$  C–H bonds adjacent to oxygen atoms. Notably, our method could be extended to larger 8-membered dioxocanes with similar efficiency under otherwise identical reaction conditions (**3l**, **3m**). As illustrated in Table 2 (bottom), the  $sp^3$  arylation could be applied independently on whether electron-rich or electron-poor aryl bromides were utilized as counterparts. The method showed an excellent chemoselectivity pattern, and esters (**2a**), nitriles (**2m**), ketones (**2o**, **2u**, **2v**), alkenes (**2k**), sulfonamides (**2j**), or amides (**2w**) could be all well-accommodated. Even heteroaryl bromides containing benzofuran, thiophen, pyridine, or quinoline cores do not interfere with productive  $sp^3$  arylation (**2q** and **2s–u**). Interestingly, no racemization was found for compounds bearing stereocenters (**2w**). More interestingly, our protocol could be extended to either vinyl bromides or unactivated alkyl halides, albeit in comparable lower yields. The latter is particularly noteworthy given the paucity of  $sp^3$ – $sp^3$  bond-forming cross-coupling reactions driven by the functionalization of unactivated alkyl  $sp^3$  C–O bonds.<sup>3</sup>

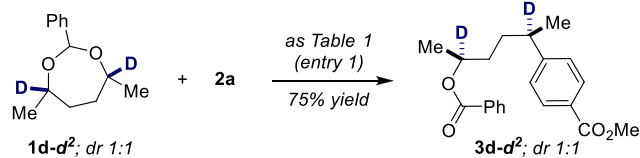
Encouraged by these results, we next conducted a series of control experiments to gain more insights into the intricacies of our  $sp^3$  C–O functionalization technique. Specifically, we studied the kinetic isotope effect by comparing the initial rates of **1a** and **1a-d** (Scheme 4, top). We observed a  $k_{\text{H}}/k_{\text{D}} = 1.0$ ,

## Scheme 4. Preliminary Mechanistic Experiments

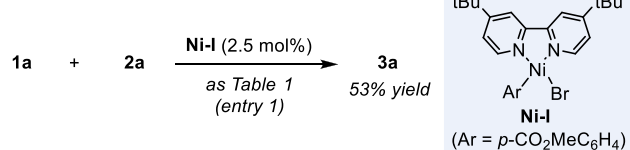
■ intermolecular kinetic isotope effect



■ arguing against competitive HAT at different  $sp^3$  C–H sites



■ reactivity of oxidative addition complex Ni-I



suggesting that  $sp^3$  C–H bond cleavage might not be involved in the rate-determining step. In addition, 1d-d<sup>2</sup> was prepared to investigate whether an erosion in deuterium content was observed in 3d-d<sup>2</sup> due to initial HAT at the  $sp^3$  C–D site followed by 1,3-HAT en route to II.<sup>18</sup> As shown, careful spectroscopic analysis revealed 3d-d<sup>2</sup> as the only observable product, advocating the notion that HAT takes place exclusively at the acetal  $sp^3$  C–H site (Scheme 4, middle).<sup>19</sup> As displayed in Scheme 4 (bottom), we found that Ni-I—easily prepared by reacting 2a with Ni(cod)<sub>2</sub> and L1 in THF—was catalytically competent en route to 3a.

In summary, we have reported a dual catalytic strategy that harnesses the potential of cyclic acetals as manifolds for enabling an atom-economical site-selective  $sp^3$  alkyl C–O functionalization. Key for success is the conformational flexibility of cyclic acetals, thus leading to an appropriate  $\sigma^*-\text{p}$  orbital overlap prior to  $\beta$ -fragmentation. The method is characterized by a broad scope across a wide number of cyclic acetals and aryl/alkyl halides, hence offering an opportunity to improve upon existing  $sp^3$  C–O functionalization scenarios.

## ■ ASSOCIATED CONTENT

### Supporting Information

The Supporting Information is available free of charge at <https://pubs.acs.org/doi/10.1021/jacs.2c04513>.

Experimental procedures, <sup>1</sup>H and <sup>13</sup>C NMR spectra for all compounds, mechanistic studies, and detailed computational data (PDF)

## ■ AUTHOR INFORMATION

### Corresponding Author

Ruben Martin – Institute of Chemical Research of Catalonia (ICIQ), The Barcelona Institute of Science and Technology, 43007 Tarragona, Spain; ICREA, 08010 Barcelona, Spain; [orcid.org/0000-0002-2543-0221](https://orcid.org/0000-0002-2543-0221); Email: [rmartinromo@icqi.es](mailto:rmartinromo@icqi.es)

### Authors

Ciro Romano – Institute of Chemical Research of Catalonia (ICIQ), The Barcelona Institute of Science and Technology,

43007 Tarragona, Spain; [orcid.org/0000-0001-7957-2316](https://orcid.org/0000-0001-7957-2316)

Laura Talavera – Institute of Chemical Research of Catalonia (ICIQ), The Barcelona Institute of Science and Technology, 43007 Tarragona, Spain; Departament de Química Analítica i Química Orgànica, Universitat Rovira i Virgili, 43007 Tarragona, Spain; [orcid.org/0000-0002-7621-5433](https://orcid.org/0000-0002-7621-5433)

Enrique Gómez-Bengoia – Department of Organic Chemistry I, Universidad País Vasco, UPV/EHU, 20080 San Sebastian, Spain; [orcid.org/0000-0002-8753-3760](https://orcid.org/0000-0002-8753-3760)

Complete contact information is available at: <https://pubs.acs.org/10.1021/jacs.2c04513>

## Author Contributions

<sup>†</sup>C.R. and L.T. contributed equally to this work

## Notes

The authors declare no competing financial interest.

## ■ ACKNOWLEDGMENTS

We thank ICIQ, FEDER/MCI-AEI/PGC2018-096839-B-I00, MCIN-PID2019-110008GB-I00, European Research Council (ERC) under European Union's Horizon 2020 research and innovation program (Grant Agreement No. 883756) for financial support. E.G.-B. thanks SGIker (UPV/EHU) for providing human and computational resources. C.R. thanks the European Union's Horizon 2020 and innovation program under the Marie Skłodowska-Curie grant agreement (839980).

## ■ REFERENCES

- For selected reviews: (a) Cornella, J.; Zarate, C.; Martin, R. Metal-catalyzed Activation of Ethers via C–O Bond Cleavage: a New Strategy for Molecular Diversity. *Chem. Soc. Rev.* **2014**, *43*, 8081–8097. (b) Tobisu, M.; Chatani, N. Cross-couplings Using Aryl Ethers via C–O Bond Activation Enabled by Nickel Catalysts. *Acc. Chem. Res.* **2015**, *48*, 1717–1726. (c) Su, B.; Cao, Z.-C.; Shi, Z.-J. Exploration of Earth-Abundant Transition Metals (Fe, Co, and Ni) as Catalysts in Unreactive Chemical Bond Activations. *Acc. Chem. Res.* **2015**, *48*, 886–896. (d) Zeng, H.; Qiu, Z.; Domínguez-Huerta, A.; Hearne, Z.; Chen, Z.; Li, C.-J. An Adventure in Sustainable Cross-Coupling of Phenols and Derivatives via Carbon–Oxygen Bond Cleavage. *ACS Catal.* **2017**, *7*, 510–519. (e) Tobisu, M. C–O Bond Transformations. In *Nickel Catalysis in Organic Synthesis*; Ogoshi, S., Ed.; Wiley-VCH: 2020; pp 123–149. (f) Boit, T. B.; Bulger, A. S.; Dander, J. E.; Garg, N. K. Activation of C–O and C–N Bonds Using Non-Precious Metal Catalysis. *ACS Catal.* **2020**, *10*, 12109–12126.
- Selected examples of alkyl  $sp^3$  C–O cleavage as oxalates derivatives: (a) Zhang, X.; MacMillan, D. W. C. Alcohols as Latent Coupling Fragments for Metalla-photo-redox Catalysis:  $sp^3 - sp^2$  Cross-Coupling of Oxalates with Aryl Halides. *J. Am. Chem. Soc.* **2016**, *138*, 13862–13865. (b) Ye, Y.; Chen, H.; Sessler, J. L.; Gong, H. Zn-Mediated Fragmentation of Tertiary Alkyl Oxalates Enabling Formation of Alkylated and Arylated Quaternary Carbon Centers. *J. Am. Chem. Soc.* **2019**, *141*, 820–824. (c) Gonzalez-Esguevillas, M.; Miró, J.; Jeffrey, J. L.; MacMillan, D. W. C. Photoredox-catalyzed Deoxyfluorination of Activated Alcohols with Selectfluor. *Tetrahedron* **2019**, *75*, 4222–4227. (d) Li, H.; Guo, L.; Feng, X.; Huo, L.; Zhu, S.; Chu, L. Sequential C–O Decarboxylative Vinylation/C–H Arylation of Cyclic Oxalates via a Nickel-catalyzed Multicomponent Radical Cascade. *Chem. Sci.* **2020**, *11*, 4904–4910.
- Example of alkyl  $sp^3$  C–O cleavage as benzoxazole derivatives: (a) Amos, S. G. E.; Cavalli, D.; Le Vaillant, F.; Waser, J. Direct Photoexcitation of Ethynylbenziodoxolones: An Alternative to Photocatalysis for Alkynylation Reactions. *Angew. Chem., Int. Ed.* **2021**, *60*, 23827–23834. (b) Sakai, H. A.; MacMillan, D. W. C. Nontraditional Fragment Couplings of Alcohols and Carboxylic

Acids: C(sp<sup>3</sup>)-C(sp<sup>3</sup>) Cross-Coupling via Radical Sorting. *J. Am. Chem. Soc.* **2022**, *144*, 6185–6192.

(4) Selected examples of alkyl sp<sup>3</sup> C–O cleavage as organophosphorous derivatives: (a) Zhang, L.; Koreeda, M. Radical Deoxygenation of Hydroxyl Groups via Phosphites. *J. Am. Chem. Soc.* **2004**, *126*, 13190–13191. (b) Li, Z.; Sun, W.; Wang, X.; Li, L.; Zhang, Y.; Li, C. Electrochemically Enabled, Nickel-Catalyzed Dehydroxylative Cross Coupling of Alcohols with Aryl Halides. *J. Am. Chem. Soc.* **2021**, *143*, 3536–3543.

(5) Selected examples of alkyl sp<sup>3</sup> C–O cleavage as sulfates derivatives: (a) Yang, C.-T.; Zhang, Z.-Q.; Liang, J.; Liu, J.-H.; Lu, X.-Y.; Chen, H.-H.; Liu, L. Copper-Catalyzed Cross-Coupling of Nonactivated Secondary Alkyl Halides and Tosylates with Secondary Alkyl Grignard Reagents. *J. Am. Chem. Soc.* **2012**, *134*, 11124–11127. (b) Eno, M. S.; Lu, A.; Morken, J. P. Nickel-Catalyzed Asymmetric Kumada Cross-Coupling of Symmetric Cyclic Sulfates. *J. Am. Chem. Soc.* **2016**, *138*, 7824–7827. (c) Duan, J.; Du, Y.-F.; Pang, X.; Shu, X.-Z. Ni-catalyzed Cross-electrophile Coupling between Vinyl/aryl and Alkyl Sulfonates: Synthesis of Cycloalkenes and Vodification of Peptides. *Chem. Sci.* **2019**, *10*, 8706–8712. (d) Komeyama, K.; Michiyuki, T.; Osaka, I. Nickel/Cobalt-Catalyzed C(sp<sup>3</sup>)-C(sp<sup>3</sup>) Cross-Coupling of Alkyl Halides with Alkyl Tosylates. *ACS Catal.* **2019**, *9*, 9285–9291. (e) Sanford, A. B.; Thane, T. A.; McGinnis, T. M.; Chen, P.-P.; Hong, X.; Jarvo, E. R. Nickel-Catalyzed Alkyl-Alkyl Cross-Electrophile Coupling Reaction of 1,3-Dimesylates for the Synthesis of Alkylcyclopropanes. *J. Am. Chem. Soc.* **2020**, *142*, 5017–5023. (f) Zhang, F.; Wang, Y.; Wang, Y.; Pan, Y. Electrochemical Deoxygenative Thiolation of Preactivated Alcohols and Ketones. *Org. Lett.* **2021**, *23*, 7524–7528. (g) Gu, Y.; Yin, H.; Wakeling, M.; An, J.; Martin, R. Defunctionalization of sp<sup>3</sup> C–Heteroatom and sp<sup>3</sup> C–C Bonds Enabled by Photoexcited Triplet Ketone Catalysts. *ACS Catal.* **2022**, *12*, 1031–1036.

(6) For additional examples on the functionalization of other alkyl sp<sup>3</sup> C–O bonds, see: (a) Barton, D. H. R.; McCombie, S. W. A New Method for the Deoxygenation of Secondary Alcohols. *J. Chem. Soc., Perkin Trans. 1* **1975**, *16*, 1574–1585. (b) Herrmann, J. M.; König, B. Reductive Deoxygenation of Alcohols: Catalytic Methods Beyond Barton-McCombie Deoxygenation. *Eur. J. Org. Chem.* **2013**, *2013*, 7017–7027. (c) Friese, F. W.; Studer, A. Deoxygenative Borylation of Secondary and Tertiary alcohols. *Angew. Chem., Int. Ed.* **2019**, *58*, 9561–9564. (d) Zhang, K.; Chang, L.; An, Q.; Wang, X.; Zuo, Z. Dehydroxymethylation of Alcohols Enabled by Cerium Photocatalysis. *J. Am. Chem. Soc.* **2019**, *141*, 10556–10564. (e) Kariofillis, S. K.; Shields, B. J.; Tekle-Smith, M. A.; Zacuto, M. J.; Doyle, A. G. Nickel/Photoredox-Catalyzed Methylation of (Hetero)aryl Chlorides Using Trimethyl Orthoformate as a Methyl Radical Source. *J. Am. Chem. Soc.* **2020**, *142*, 7683–7689. (f) Cao, D.; Chen, Z.; Lv, L.; Zeng, H.; Peng, Y.; Li, C.-J. Light-Driven Metal-Free Direct Deoxygenation of Alcohols under Mild Conditions. *iScience* **2020**, *23*, 101419. (g) Xie, H.; Guo, J.; Wang, Y.-G.; Wang, K.; Guo, P.; Su, P.-F.; Wang, X.; Shu, X.-Z. Radical Dehydroxylative Alkylation of Tertiary Alcohols by Ti Catalysis. *J. Am. Chem. Soc.* **2020**, *142*, 16787–16794. (h) Cook, A.; MacLean, H.; St. Onge, P.; Newman, S. G. Nickel-Catalyzed Reductive Deoxygenation of Diverse C–O Bond-Bearing Functional Groups. *ACS Catal.* **2021**, *11*, 13337–13347. (i) Xie, H.; Wang, S.; Wang, Y.; Guo, P.; Shu, X.-Z. Ti-Catalyzed Reductive Dehydroxylative Vinylation of Tertiary Alcohols. *ACS Catal.* **2022**, *12*, 1018–1023.

(7) Luo, Y.-R. Tabulated BDEs of C–H bonds. *Handbook of Bond Dissociation Energies in Organic Compounds*; CRC Press: 2002; pp 11–93.

(8) (a) For excellent reviews on the topic: Twilton, J.; Le, C. C.; Zhang, P.; Shaw, M. H.; Evans, R. W.; MacMillan, D. W. C. The Merger of Transition Metal and Photocatalysis. *Nat. Rev. Chem.* **2017**, *1*, 0052. (b) Chan, A. Y.; Perry, I. B.; Bissonnette, N. B.; Buksh, B. F.; Edwards, G. A.; Frye, L. I.; Garry, O. L.; Lavagnino, M. N.; Li, B. X.; Liang, Y.; Mao, E.; Millet, A.; Oakley, J. V.; Reed, N. L.; Sakai, H. A.; Seath, C. P.; MacMillan, D. W. C. Metallaphotoredox: The Merger of

Photoredox and Transition Metal Catalysis. *Chem. Rev.* **2022**, *122*, 1485–1542.

(9) While this manuscript was under preparation, Doyle reported the utilization of acyclic, symmetrical acetals for sp<sup>3</sup> C–O cleavage. Kariofillis, S. K.; Jiang, S.; Žuraňski, A. M.; Gandhi, S. S.; Martinez Alvarado, J. I.; Doyle, A. G. Using Data Science To Guide Aryl Bromide Substrate Scope Analysis in a Ni/Photoredox-Catalyzed Cross-Coupling with Acetals as Alcohol-Derived Radical Sources. *J. Am. Chem. Soc.* **2022**, *144*, 1045–1055.

(10) (a) Nakamura, C. E.; Whited, G. M. Metabolic engineering for the Microbial Production of 1,3-propanediol. *Curr. Opin. Biotechnol.* **2003**, *14*, 454–459. (b) Yim, H.; Haselbeck, R.; Niu, W.; Pujol-Baxley, C.; Burgard, A.; Boldt, J.; Khandurina, J.; Trawick, J. D.; Osterhout, R. E.; Stephen, R.; Estadilla, J.; Teisan, S.; Schreyer, H. B.; Andrae, S.; Yang, T. H.; Lee, S. Y.; Burk, M. J.; Van Dien, S. Metabolic Engineering of *Escherichia Coli* for Direct Production of 1,4-butanediol. *Nat. Chem. Biol.* **2011**, *7*, 445–452. (c) Zeng, A. P.; Sabra, W. Microbial Production of Diols as Platform Chemicals: Recent Progresses. *Curr. Opin. Biotechnol.* **2011**, *22*, 749–757. (d) Jang, Y.-S.; Kim, B.; Shin, J. H.; Choi, Y. J.; Choi, S.; Song, C. W.; Lee, J.; Park, H. G.; Lee, S. Y. Bio-based Production of C2–C6 Platform Chemicals. *Biotechnol. Bioeng.* **2012**, *109*, 2437–2459. (e) Sabra, W.; Groeger, C.; Zeng, A. P. Microbial Cell factories for Diol Production. *Adv. Biochem. Eng. Biotechnol.* **2016**, *155*, 165–197. (f) Zhang, Y.; Liu, D.; Chen, Z. Production of C2–C4 Diols from Renewable Bioresources: new Metabolic Pathways and Metabolic Engineering Strategies. *Biotechnol. Biofuels* **2017**, *10*, 299. (g) Palkovits, R.; Delidovich, I. Efficient Utilization of Renewable Feedstocks: the Role of Catalysis and Process Design. *Philos. Trans. R. Soc.* **2018**, *376*, 20170064. (h) Wang, J.; Li, C.; Zou, Y.; Yan, Y. Bacterial Synthesis of C3–C5 Diols via Extending Amino Acid Catabolism. *Proc. Natl. Acad. Sci.* **2020**, *117*, 19159–19167.

(11) Nielsen, M. K.; Shields, B. J.; Liu, J.; Williams, M. J.; Zacuto, M. J.; Doyle, A. G. Mild, Redox-Neutral Formylation of Aryl Chlorides via Photocatalytic Generation of Chlorine Radicals. *Angew. Chem., Int. Ed.* **2017**, *56*, 7191–7194.

(12) All structures were optimized using Gaussian 16 at the M06-2X/6-311++G(d,p) level, introducing solvation factors with the IEF-PCM method (2-methyl-2-propanol as solvent). For more details, see [Supporting Information](#).

(13) For selected publications: (a) Zarate, C.; Nakajima, M.; Martin, R. A Mild and Ligand-Free Ni-Catalyzed Silylation via C–OME Cleavage. *J. Am. Chem. Soc.* **2017**, *139*, 1191–1197. (b) Somerville, R.; Hale, L.; Gomez-Bengoia, E.; Burés, J.; Martin, R. Intermediacy of Ni–Ni Species in sp<sup>2</sup> C–O Bond Cleavage of Aryl Esters: Relevance in Catalytic C–Si Bond Formation. *J. Am. Chem. Soc.* **2018**, *140*, 8771–8780. (c) Day, C. S.; Somerville, R. J.; Martin, R. Deciphering the Dichotomy Exerted by Zn(II) in the Catalytic sp<sup>2</sup> C–O Bond Functionalization of Aryl Esters at the Molecular Level. *Nat. Catal.* **2021**, *4*, 124–133. (d) Shen, Y.; Gu, Y.; Martin, R. sp<sup>3</sup> C–H Arylation and Alkylation Enabled by the Synergy of Triplet Excited Ketones and Nickel Catalysts. *J. Am. Chem. Soc.* **2018**, *140*, 12200–12209. (e) Rand, A. W.; Yin, H.; Xu, L.; Giacoboni, J.; Martin-Montero, R.; Romano, C.; Montgomery, J.; Martin, R. Dual Catalytic Platform for Enabling sp<sup>3</sup> a C–H Arylation & Alkylation of Benzamides. *ACS Catal.* **2020**, *10*, 4671–4676. (f) Cong, F.; Lv, X.-Y.; Day, C. S.; Martin, R. Dual Catalytic Strategy for Forging sp<sup>2</sup>–sp<sup>3</sup> and sp<sup>3</sup>–sp<sup>3</sup> Architectures via β-scission of Aliphatic Alcohol Derivatives. *J. Am. Chem. Soc.* **2020**, *142*, 20594–20599.

(14) Despite extensive investigations by varying all experimental parameters, we were not able to detect even traces of products arising from sp<sup>3</sup> C–O cleavage by using either six-membered 2-phenyl-1,3-dioxane or five-membered 2-phenyl-1,3-dioxolane as substrates. While this empirical observation is in full agreement with our DFT studies, thus confirming the need for conformational flexibility in the targeted sp<sup>3</sup> C–O cleavage, it is worth noting that a single example has been described by using the latter in ref 9, albeit in low yields.

(15) See [Supporting Information](#) for details.

(16) For selected photoinduced processes proposed to operate via bromine radicals: (a) Tanko, J.; Sadeghipour, M. Functionalization of Hydrocarbons by a New Free Radical Based Condensation Reaction. *Angew. Chem., Int. Ed.* **1999**, *38*, 159–161. (b) Kippo, T.; Kimura, Y.; Maeda, A.; Matsubara, H.; Fukuyama, T.; Ryu, I. Radical Vinylation of Dioxolanes and N-acylpyrrolidines Using Vinyl Bromides. *Org. Chem. Front.* **2014**, *1*, 755–758. (c) Kippo, T.; Kimura, Y.; Ueda, M.; Fukuyama, T.; Ryu, I. Bromine-Radical-Mediated Synthesis of  $\beta$ -functionalized  $\beta,\gamma$ - and  $\delta,\epsilon$ -Unsaturated Ketones via C–H Functionalization of Aldehydes. *Synlett* **2017**, *28*, 1733–1737. (d) Ueda, M.; Maeda, A.; Hamaoka, K.; Sasano, M.; Fukuyama, T.; Ryu, I. Bromine-Radical Mediated Site-selective Allylation of C(sp<sup>3</sup>)–H Bonds. *Synthesis* **2019**, *51*, 1171–1177. (e) Jia, P.; Li, Q.; Poh, W. C.; Jiang, H.; Liu, H.; Deng, H.; Wu, J. Light-Promoted Bromine Radical-Mediated Selective Alkylation and Amination of Unactivated C(sp<sup>3</sup>)–H Bonds. *Chem.* **2020**, *6*, 1766–1776. (f) Talukdar, R. Tracking Down the Brominated Single Electron Oxidants in Recent Organic Red-ox Transformations: Photolysis and Photocatalysis. *Org. Biomol. Chem.* **2020**, *18*, 8294–8345. (g) Chen, D.-F.; Chrisman, C. H.; Miyake, G. M. Bromine Radical Catalysis by Energy Transfer Photosensitization. *ACS Catal.* **2020**, *10*, 2609–2614. (h) Santos, M. S.; Correa, A. G.; Paixão, M. W.; König, B. C(sp<sup>3</sup>)–C(sp<sup>3</sup>) Cross Coupling of Alkyl Bromides and Ethers Mediated by Metal and Visible Light Photoredox Catalysis. *Adv. Synth. Catal.* **2020**, *362*, 2367–2372. (i) Wang, H.; Liu, H.; Wang, M.; Huang, M.; Shi, X.; Wang, T.; Cong, X.; Yan, J.; Wu, J. Bromine Radical as a Visible-Light-Mediated Polarity-Reversal Catalyst. *iScience* **2021**, *24*, 102693.

(17) Ingold, K. U.; DiLabio, G. A. Bond Strengths: the Importance of Hyperconjugation. *Org. Lett.* **2006**, *8*, 5923–5925.

(18) Yang, B.; Li, S.-J.; Wang, Y.; Lan, Y.; Zhu, S. Hydrogen Radical-shuttle (HRS)-enabled Photoredox Synthesis of Indanones via Decarboxylative Annulation. *Nat. Commun.* **2021**, *12*, 5257.

(19) As expected, reaction of **1a** with **2a** in the presence of TEMPO ((2,2,6,6-tetramethylpiperidin-1-yl)oxyl) resulted in ~20% of **3a-TEMPO** (as judged by GC-MS of the crude mixtures). No traces of **3a** were detected in the crude mixtures, thus indirectly confirming the radical nature of the process. Attempts at isolating **3a-TEMPO** in pure form were met with failure. See ref 15.